

# 低频振幅算法功能磁共振成像对不同病因内侧颞叶癫痫的研究

魏渭 张志强 许强 黄育斌 卢光明 谭启富

**【摘要】 目的** 研究不同病理基础内侧颞叶癫痫患者异常脑功能活动分布模式的差异,探讨异常活动脑区在内侧颞叶癫痫发病过程中的病理生理学机制。**方法** 采用基于低频振幅(ALFF)的静息态fMRI技术,分别对30例单侧海马硬化性内侧颞叶癫痫(mTLE-HS)和30例单侧占位性内侧颞叶癫痫(mTLE-OL)患者进行研究,并与30例性别和年龄相匹配的正常对照者进行比较。经代价函数预处理图像后,REST软件计算全脑低频振幅均值并作归一化处理获得mALFF值,两样本t检验依次对3组被试mALFF值进行比较,对比mTLE-HS和mTLE-OL颞叶外脑区mALFF值变化,并分析mALFF值改变脑区与癫痫病程之间关联性。**结果** 静息态下,mTLE-HS组和mTLE-OL组患者均呈现颞叶外mALFF值改变,但异常脑区分布模式不同。与mTLE-HS组相比,mTLE-OL组患者mALFF值增强区域位于双侧顶下叶、楔前叶、角回、扣带中后回和对侧颞中回;mALFF值减弱区域为对侧中央后回、双侧枕中回和小脑(均 $P < 0.05$ ,AlphaSim校正),提示mTLE-HS较mTLE-OL脑默认网络受抑制程度更为严重。mTLE-HS患者局部mALFF值与癫痫病程无明显关联性,而mTLE-OL患者双侧扣带中后回mALFF值与病程呈正相关( $r = 0.687, P = 0.000$ ),双侧前扣带回与病程呈负相关( $r = -0.621, P = 0.000$ )。**结论** 不同病理基础内侧颞叶癫痫存在不同的异常脑功能活动分布模式,提示二者潜在的病理生理学机制可能不同,验证了mTLE-HS是一种特异性癫痫类型。

**【关键词】** 癫痫,颞叶; 磁共振成像; 海马

## An fMRI study of mesial temporal lobe epilepsy with different pathological basis using amplitude of low-frequency fluctuation analysis

WEI Wei<sup>1</sup>, ZHANG Zhi-qiang<sup>1</sup>, XU Qiang<sup>1</sup>, HUANG Yu-bin<sup>1</sup>, LU Guang-ming<sup>1</sup>, TAN Qi-fu<sup>2</sup>

<sup>1</sup>Department of Medical Imaging, <sup>2</sup>Department of Neurosurgery, Jinling Hospital, Nanjing University School of Medicine, Nanjing 210002, Jiangsu, China

Corresponding author: LU Guang-ming (Email: cjr.luguangming@vip.163.com)

**【Abstract】 Objective** To study the distinction of abnormal brain activity in mesial temporal lobe epilepsy (mTLE) with hippocampal sclerosis (HS) or other pathological basis, and to discuss their underlying pathophysiological mechanism in mTLE. **Methods** Thirty mTLE patients with unilateral hippocampal sclerosis (mTLE-HS) and 30 mTLE patients with occupying lesion in unilateral temporal lobe (mTLE-OL) were investigated by comparing with 30 age- and sex-matched healthy subjects. MRI data were collected using a Siemens 3.0T scanner, and all of the participants were studied using amplitude of low-frequency fluctuation (ALFF) analysis of resting state fMRI. A cost - function modification was used for image preprocessing, then the difference of extratemporal mALFF changes between the two groups of mTLE patients were analyzed with two-sample t test, and the correlation between mALFF and epilepsy duration of mTLE were also investigated. **Results** In the resting state, mTLE-HS patients and mTLE-OL patients all showed significant changes in mALFF in extratemporal structures, but the distribution patterns of changes in brain were different. Compared with mTLE-HS, the mTLE-OL patients showed increased mALFF in bilateral inferior parietal lobes, precuneus, angular gyrus, middle and posterior cingulate gyrus and

doi:10.3969/j.issn.1672-6731.2014.11.008

基金项目:国家自然科学基金资助项目(项目编号:81271553)

作者单位:210002 南京大学医学院附属金陵医院影像科 南京军区南京总医院医学影像科(魏渭、张志强、许强、黄育斌、卢光明),神经外科(谭启富)

通讯作者:卢光明(Email:cjr.luguangming@vip.163.com)

contralateral middle temporal gyrus, while mALFF reducing was observed in contralateral postcentral gyrus, bilateral middle occipital gyrus and cerebellum ( $P < 0.05$ , AlphaSim corrected), that is to say, the default mode network (DMN) in mTLE-HS were inhibited more seriously than in mTLE-OL patients. Correlation analysis showed that no significant correlation was found between mALFF and epilepsy duration in mTLE-HS patients; mALFF in bilateral middle and posterior cingulate gyrus was positively correlated with epilepsy duration in mTLE-OL patients ( $r = 0.687$ ,  $P = 0.000$ ), while mALFF in bilateral anterior cingulate gyrus was negatively correlated with epilepsy duration ( $r = -0.621$ ,  $P = 0.000$ ). **Conclusions** mTLE with different pathological basis showed different distribution patterns of abnormal brain function, which indicated that their latent pathophysiological mechanism might be different, further confirming mTLE-HS was a specific type of epilepsy.

**【Key words】** Epilepsy, temporal lobe; Magnetic resonance imaging; Hippocampus

This study was supported by National Natural Science Foundation of China (No. 81271553).

内侧颞叶癫痫(mTLE)为临床常见的药物难治性癫痫类型,其特征性病理学基础是海马硬化(HS)。此外,占位性内侧颞叶癫痫(mTLE-OL),如低级别胶质瘤、脉络膜裂囊肿或皮质发育不良等,也是重要癫痫类型。一般而言,不同病因所致的内侧颞叶癫痫具有不同的临床特点,可能是不同疾病类型。海马硬化性内侧颞叶癫痫(mTLE-HS)具有一定特异性<sup>[1]</sup>,既往多有高热惊厥史或早期脑血管事件<sup>[2]</sup>,且存在较严重的认知损害<sup>[1]</sup>;而mTLE-OL更易发生复杂部分性发作或继发全面性发作<sup>[3]</sup>。癫痫网络研究提示,病灶以外的诸多脑结构亦可参与癫痫活动的产生和传播,因此除原发病灶外,可能还存在更广泛的脑结构或功能损害,这可能即是内侧颞叶癫痫表现出不同临床特点的病理生理学基础<sup>[4]</sup>。基于低频振幅(ALFF)的血氧水平依赖性功能磁共振成像(BOLD-fMRI)可在无同步脑电图检查的情况下对自发性异常脑电活动进行探测,我们采用该项技术对mTLE-HS和mTLE-OL进行研究,以观察二者脑功能活动改变的分布模式,并探讨其可能的病理生理学机制。

## 对象与方法

### 一、研究对象

1. 纳入标准 (1)参照2001年国际抗癫痫联盟(ILAE)分类标准,诊断明确的颞叶癫痫,包括复杂部分性发作等典型颞叶癫痫症状。(2)常规或长程脑电图显示单侧颞叶发作期或发作间期癫痫波。(3)常规MRI显示单侧海马硬化或颞叶占位性病变,病灶直径<2 cm。(4)所有受试者于检查前均获得知情同意,并签署知情同意书。

2. 一般资料 选择2009年8月~2013年8月在

南京军区南京总医院就诊并符合纳入标准的内侧颞叶癫痫患者共计60例,mTLE-HS和mTLE-OL各30例。(1)mTLE-HS组:30例患者,男性17例,女性13例;年龄15~48岁,平均( $30.40 \pm 10.60$ )岁;病程0.17~25年,平均( $8.24 \pm 7.06$ )年;病灶居左侧14例、右侧16例。(2)mTLE-OL组:30例患者,男性19例,女性11例;年龄15~56岁,平均( $30.67 \pm 11.60$ )岁;病程0.50~26年,平均( $8.57 \pm 7.53$ )年。病灶居左侧者14例、右侧16例,其中13例经病理检查证实诊断(表1)。(3)正常对照组:以30例同期在我院进行体检的健康志愿者作为正常对照组,均排除神经或精神疾病,男性18例,女性12例;年龄19~40岁,平均( $28.60 \pm 7.60$ )岁。mTLE-HS组与mTLE-OL组患者性别( $\chi^2 = 0.278$ ,  $P = 0.598$ )、年龄( $t = 0.093$ ,  $P = 0.926$ )、病程( $t = 0.177$ ,  $P = 0.860$ )和病灶侧别( $\chi^2 = 0.000$ ,  $P = 1.000$ )比较,差异均无统计学意义;3组受试者性别( $\chi^2 = 0.278$ ,  $P = 0.870$ )和年龄( $F = 0.374$ ,  $P = 0.689$ )比较,差异无统计学意义。

### 二、研究方法

1. 数据采集 采用德国Siemens公司生产的Magnetom Trio Tim 3.0T超高场强MRI扫描仪进行数据采集。受试者闭目平卧,尽量不做意向性思维活动,海绵垫固定头部。采集序列为基于梯度回波序列(GRE)的单次激发回波平面成像(EPI),重复时间(TR)2000 ms、回波时间(TE)30 ms,扫描视野(FOV)240 mm×240 mm,矩阵64×64,反转角度900°,共采集250个时间点,扫描层厚4 mm、层间距0.40 mm,共30层。同时采集磁化准备快速梯度回波(MPRAGE)序列获取三维T<sub>1</sub>WI(3D-T<sub>1</sub>WI)图像。

2. 数据处理 (1)静息态fMRI(rs-fMRI)和3D-T<sub>1</sub>WI数据格式转换和数据左右翻转:采用MRIcroN

**表1** mTLE-OL组患者病理类型**Table 1.** The pathological types of mTLE-OL patients

Type	N	Lateralization
Cavernous hemangioma	10	L7R3
Glioma or gliosis	8	L2R6
Choroid plexus cyst	6	L2R4
DNT	2	L1R1
Cortical dysplasia	2	L1R1
AVM	1	R1
Unknown	1	R1

DNT, dysembryoplastic neuroepithelial tumor, 胚胎发育不良性神经上皮肿瘤; AVM, arteriovenous malformation, 动-静脉畸形; L, left, 左侧; R, right, 右侧

软件 (<http://www.cabiatl.com/micro/micro/micro.html>) 将 DICOM 数据转换为 NIFTI\_1 格式。因被试数目较少, 将病灶位于右侧患者的图像进行左右翻转, 即右侧图像翻转至左侧。(2)调整原点: 将静息态 fMRI 和 3D-T<sub>1</sub>WI 的 NIFTI\_1 数据逐个轻微旋转平移, 调整原点至前后联合, 以减少后续分析时的误差。同时, 将二者数据配准, 便于后续处理。(3)在 3D-T<sub>1</sub>WI 数据上创建代价 mask 区: 采用个体空间手动勾画病灶区域, 保留占位 mask。采用 MRICroN 软件创建全脑去头皮 mask, 再减去占位 mask, 即创建去除占位后的全脑 mask 作为代价 mask。(4)标准化: 采用 SPM8 软件 (<http://www.fil.ion.ucl.ac.uk/spm/>) 中的 normalise 功能, 以代价函数配准方式通过代价 mask 将每例患者的结构数据(3D-T<sub>1</sub>WI)配准至标准空间即加拿大蒙特利尔神经病学研究所(MNI)空间, 同时获得该被试 MNI 空间的代价 mask。(5)创建 MNI 空间特异性组平均 T<sub>1</sub>WI 模板和代价 mask: 重复第(3)和(4)步获得所有患者的 MNI 空间结构图像和 MNI 空间代价 mask 图像, 平均化结构图像, 同时创建总体代价 mask 图像。(6)创建 MNI 空间特异性组平均灰质、白质和脑脊液模板: 采用代价函数通过特异性组水平代价 mask 图像, 分割获得特异性组水平之灰质、白质和脑脊液模板。(7)重分割并将 T<sub>1</sub>WI 图像重配准: 采用代价函数方式, 以第(6)步获取的特异性组水平灰质、白质和脑脊液模板为基准, 结合个体空间的代价 mask, 分割其结构图像 T<sub>1</sub>WI, 获取 T<sub>1</sub>WI 向 MNI 空间的变换矩阵 T。将变换矩阵 T 写给第(2)步配准后的静息态 fMRI 数据, 并重采样成 3 mm × 3 mm × 3 mm, 得到 MNI 空间静息态 fMRI 数据。(8)平滑: 以半高全宽(FWHM)为

8 mm 进行高斯平滑。(9)滤波: 行 0.01~0.10 Hz 带通滤波以消除呼吸、心脏搏动和低频噪声。(10)计算 ALFF: 采用 REST 软件计算信号振幅平均值, 即 BOLD 信号变化强度, 得到振幅之统计参数脑图。(11)M 值化: 全脑体素除以全脑均值作归一化处理获得 mALFF 值, 以去除个体均值差异。(12)正常被试处理: 数据提取后, 采用 DPARSFA 软件进行处理, 包括时间校正、头动校正; 据 DPARSFA 软件提供的“T<sub>1</sub>WI 统一分割标准化”采样成 3 mm × 3 mm × 3 mm; 其后步骤同第(8)~(11)步。

3. 统计分析方法 采用 SPM8 软件对上述处理后的数据进行分析, 分别对 3 组 mALFF 统计参数脑图依次行两样本 t 检验, 采用 AlphaSim 法对结果进行多重校正( $P < 0.05$ , 体素  $> 2040$ ), 并将结果叠加于标准结构模板。由于颞叶占位性病变在预处理过程中被遮盖, 因此本研究仅观察内侧颞叶癫痫患侧颞叶外脑区。最终提取 mTLE-HS 和 mTLE-OL 患者异常脑区 mALFF 值, 与癫痫病程行 Pearson 相关分析, 阈值水平以  $P \leq 0.05$  为差异具有统计学意义。

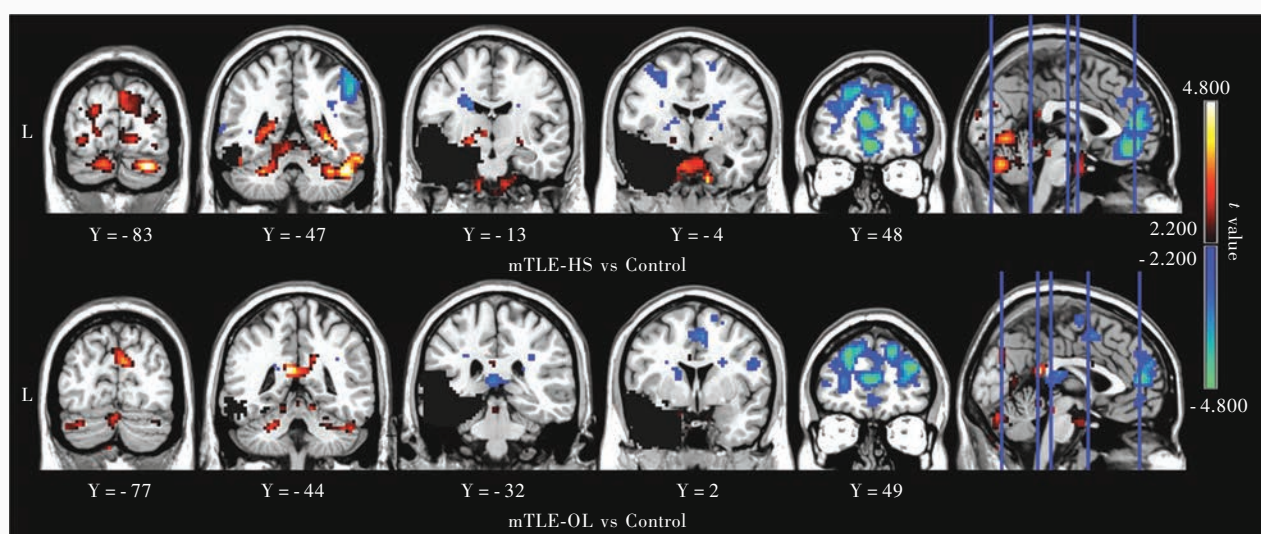
## 结 果

两样本 t 检验结果显示, 与正常对照组相比, mTLE-HS 组患者 mALFF 值明显增强区域位于双侧小脑、舌状回、距状回、楔状回、丘脑和对侧颞下回; mALFF 值减弱区域位于双侧额叶和前扣带回、患侧壳核和中央前回、对侧顶下回和角回(图 1, 表 2)。与正常对照组相比, mTLE-OL 组患者双侧小脑、扣带中后回、楔状回和舌状回 mALFF 值明显增强; 而双侧额中上回、辅助运动区、前扣带回和胼胝体压部 mALFF 值减弱(图 1, 表 3)。与 mTLE-HS 组相比, mTLE-OL 组患者 mALFF 值增强区域分别位于双侧顶下叶、楔前叶、角回、扣带中后回和对侧颞中回; mALFF 值减弱区域为对侧中央后回、双侧枕中回和小脑(图 2)。

Pearson 相关分析结果显示, 双侧扣带中后回 mALFF 值与 mTLE-OL 患者癫痫病程呈正相关( $r = 0.687, P = 0.000$ ), 而双侧前扣带回与病程呈负相关( $r = -0.621, P = 0.000$ )。

## 讨 论

本研究结果显示, mTLE-HS 与 mTLE-OL 具有不同的异常脑功能活动分布模式, 从神经影像学角度



mTLE-HS, mesial temporal lobe epilepsy-hippocampal sclerosis; 海马硬化性内侧颞叶癫痫; mTLE-OL, mesial temporal lobe epilepsy-occupying lesion, 占位性内侧颞叶癫痫; L, left, 左侧。The same as figure below

**图1** mTLE-HS组和mTLE-OL组与正常对照组患者mALFF值两样本t检验结果图:与正常对照组相比,mTLE-HS组患者mALFF值增强区域为双侧小脑(前叶、后叶)、舌状回、距状回、楔状回、丘脑和对侧颞下回(红色区域所示);mALFF值减弱区域为双侧额叶和前扣带回、患侧壳核和中央前回、对侧顶下回和角回(蓝色区域所示)。与正常对照组相比,mTLE-OL组患者mALFF值增强区域为双侧小脑(前叶、后叶)、扣带中后回、楔状回和舌状回(红色区域所示);mALFF值减弱区域为双侧额中上回、辅助运动区、前扣带回和胼胝体压部(蓝色区域所示)

**Figure 1** The upper figure showed the comparison of mALFF between mTLE-HS patients and controls using two-sample *t* test. In comparison with the controls, the mTLE-HS patients showed increased mALFF in bilateral cerebellum (anterior and posterior lobes), lingual gyrus, cryptocalcarine gyrus, cuneus gyrus, thalamus and contralateral inferior temporal gyrus (red areas indicate), while the regions showing decreased mALFF included bilateral frontal lobes and anterior cingulate cortex, ipsilateral putamen and precentral gyrus, contralateral inferior parietal gyrus and angular gyrus (blue areas indicate). The lower figure showed comparison of mALFF between mTLE-OL patients and controls using two-sample *t* test. In comparison with the controls, the mTLE-OL patients showed increased mALFF in bilateral cerebellum (anterior and posterior lobes), middle and posterior cingulate cortex, cuneus and lingual gyrus (red areas indicate), while decreased mALFF was observed in bilateral middle and superior frontal gyrus, supplementary motor areas, anterior cingulate cortex and splenium of corpus callosum (blue areas indicate).

**表2** mTLE-HS组患者mALFF值改变脑区分析\*

**Table 2.** Regions showing abnormal mALFF in mTLE-HS patients\*

Brain region	<i>t</i> value	MNI (mm)			BA	Voxel	Brain region	<i>t</i> value	MNI (mm)			BA	Voxel
		x	y	z					x	y			
<b>Increased mALFF</b>													
R. posterior lobe of cerebellum	4.330	33	-78	-30	—	365	R. middle frontal gyrus	-2.880	42	48	15	10	891
L. posterior lobe of cerebellum	1.830	-21	-75	-30	—	275	L. middle frontal gyrus	-3.520	-24	48	27	10	738
R. anterior lobe of cerebellum	4.010	33	-48	-33	—	291	R. superior frontal gyrus	-3.800	15	51	33	9	408
L. anterior lobe of cerebellum	2.110	-24	-48	-27	—	347	L. superior frontal gyrus	-4.350	-21	36	36	9	525
R. lingual gyrus	3.270	3	-72	0	18	324	R. inferior frontal gyrus	-2.390	51	39	3	46	135
L. lingual gyrus	1.940	-18	-54	-3	19	346	L. inferior frontal gyrus	-2.240	-51	24	24	45	89
R. cryptocalcarine gyrus	2.950	27	-54	12	—	230	Bilateral anterior cingulate	-2.070	0	30	30	32	337
L. cryptocalcarine gyrus	3.110	-21	-51	9	—	222	R. inferior parietal gyrus	-2.780	48	-51	45	40	208
R. cuneus gyrus	2.840	3	-81	33	19	220	L. putamen	-2.530	-21	3	9	—	110
L. cuneus gyrus	2.230	-12	-87	27	19	95	L. precentral gyrus	-2.380	-39	-3	60	6	91
R. inferior temporal gyrus	2.620	60	-42	-18	20	189	R. angular gyrus	-2.150	36	-57	51	7	78
R. thalamus	2.050	12	-12	3	—	44							
L. thalamus	2.060	-15	-12	0	—	60							

\**P* < 0.05, for all. MNI, Montreal Neurological Institute, 加拿大蒙特利尔神经病学研究所; BA, Brodmann's area, Brodmann分区; ALFF, amplitude of low-frequency fluctuation, 低频振幅;mALFF, M值化低频振幅;R, right, 右侧;L, left, 左侧;—, unpartitioned, 未分区。The same as table below

**表3** mTLE-OL组患者mALFF值改变脑区分析\***Table 3.** Regions showing abnormal mALFF in mTLE-OL patients\*

Brain region	t value	MNI (mm)			BA	Voxel	Brain region	t value	MNI (mm)			BA	Voxel
		x	y	z					x	y	z		
<b>Increased mALFF</b>													
R. posterior lobe of cerebellum	3.090	36	-51	-33	—	211	R. middle frontal gyrus	-4.900	36	24	45	8	702
L. posterior lobe of cerebellum	2.920	-27	-45	-33	—	205	L. middle frontal gyrus	-3.890	-24	45	30	10	392
R. anterior lobe of cerebellum	2.410	24	-54	-24	—	134	R. superior frontal gyrus	-3.110	18	21	57	6	634
L. anterior lobe of cerebellum	2.210	-15	-60	-24	—	131	L. superior frontal gyrus	-4.550	-18	51	39	9	443
R. cuneus gyrus	3.750	6	-78	30	7	119	R. supplementary motor areas	-3.100	0	6	54	6	194
L. cuneus gyrus	1.850	-6	-75	27	31	56	L. supplementary motor areas	-2.970	-3	6	51	32	103
R. middle cingulate	2.170	0	-9	30	24	108	R. anterior cingulate	1.800	3	9	24	33	129
L. middle cingulate	2.030	-3	-18	33	23	61	L. anterior cingulate	2.110	-3	9	27	33	132
R. posterior cingulate	3.980	3	-42	18	29	50							
L. posterior cingulate	3.970	0	-42	21	23	59							
L. lingual gyrus	2.180	-15	-81	3	17	85							

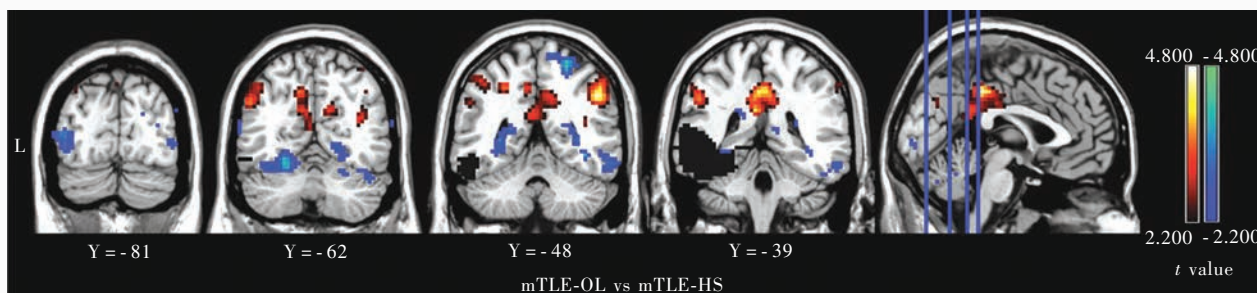


**图2** mTLE-OL组与mTLE-HS组患者mALFF值两样本t检验结果图:与mTLE-HS组相比,mTLE-OL组患者双侧顶下叶、楔前叶、角回、扣带中后回和对侧颞中回mALFF值增强(红色区域所示);对侧中央后回、双侧枕中回和小脑mALFF值减弱(蓝色区域所示)

**Figure 2** The figure showed the comparison of mALFF between mTLE-OL and mTLE-HS patients using two-sample t test. Compared with mTLE-HS patients, the mTLE-OL patients showed increased mALFF in bilateral inferior parietal lobes, precuneus, angular gyrus, middle and posterior cingulate gyrus, and contralateral middle temporal gyrus (red areas indicate), while showed decreased mALFF in contralateral postcentral gyrus, bilateral middle occipital lobes and cerebellum (blue areas indicate).

证明二者为不同的疾病类型。与mTLE-HS组相比, mTLE-OL组患者mALFF值增强区域为双侧顶下叶、楔前叶、角回、扣带中后回和对侧颞中回等脑默认网络(DMN)区域, mALFF值减弱区域为对侧中央后回、双侧枕中回和小脑。

ALFF是由我国学者Zang等<sup>[5]</sup>首次提出的反映脑局部特征的影像学诊断技术,通过计算一定时间内BOLD信号偏离基线的平均值,以反映该时间内脑自发性代谢活动之强度。癫痫是一种神经元异常同步放电的中枢神经系统疾病,可引起相应脑区BOLD信号的改变<sup>[6]</sup>,从而使ALFF信号增强,因此ALFF值增强能够间接反映癫痫活动程度,该方法的有效性已经本研究小组既往研究结果所验证<sup>[7]</sup>。

在本研究中,与正常对照组相比, mTLE-HS组患者双侧小脑、部分枕叶(包括舌状回和楔状回)、

健侧颞下回均呈现mALFF值增强,与张志强等<sup>[8]</sup>的研究结果相一致,反映上述脑区受癫痫的影响较大,揭示存在颞叶癫痫网络,从而将大脑构建为一个整体运作。此外,丘脑在癫痫的易化和播散中具有重要作用<sup>[9]</sup>,其与大脑皮质或皮质下结构具有广泛的非特异纤维连接,主要影响全面性发作。SPECT研究结果表明,内侧颞叶癫痫患者存在丘脑受累<sup>[10]</sup>,本研究也证实了丘脑在内侧颞叶癫痫中的重要作用。本研究结果还发现, mTLE-HS组患者双侧额叶和前扣带回、对侧顶下回和角回呈现mALFF值减弱,上述区域部分参与了脑默认网络<sup>[11]</sup>。

在本研究中,与正常对照组相比, mTLE-OL组患者双侧额中上回和前扣带回mALFF值减弱,提示脑默认网络受损,但与mTLE-HS组患者的mALFF分布模式不同。患者楔叶和扣带中后回mALFF值

增强,有文献报道,楔前叶与后扣带回之间存在网状环路,二者共同参与记忆活动的调节<sup>[12]</sup>,后扣带回mALFF值增强可能解释了mTLE-OL患者在复杂部分性发作和全面性发作时出现的意识丧失。

不同病理基础内侧颞叶癫痫呈现不同的mALFF值改变脑区。与mTLE-HS组相比,mTLE-OL组患者双侧顶下叶、楔前叶、角回、扣带中后回和对侧颞中回mALFF值增强,即mTLE-HS较mTLE-OL患者脑默认网络区域受抑制程度更严重。脑默认网络与人类情景记忆、内外环境监测和自我认知评价有关,发作间期的痫样放电可引起脑默认网络的中断挂起,其活动受损可能反映了癫痫患者脑高级认知功能障碍的神经病理学机制<sup>[13]</sup>。内侧颞叶癫痫患者脑默认网络区域受损见于许多fMRI研究报道<sup>[14-15]</sup>,笔者推测,发作间期痫样放电可以抑制脑默认网络中的mALFF信号强度。根据能量代谢规律,脑默认网络各区域在静息态下呈现高能量代谢,而在工作记忆时为低代谢,随着记忆任务的增加,能量代谢减弱程度相应增加<sup>[16]</sup>,即本研究mTLE-HS组患者脑默认网络各区域具有更低的代谢水平、认知损害程度更严重,与李军杰等<sup>[17]</sup>和王秀等<sup>[18]</sup>的研究结果相一致。两组患者的认知水平在临床表现上是否存在差异,尚待进一步研究加以证实。此外,两种病理基础内侧颞叶癫痫均出现小脑mALFF值增强,可能与癫痫发作过程中身体的不自主运动有关<sup>[19]</sup>,也有研究认为,小脑mALFF值增强与代偿引起的神经自发性活动增多有关<sup>[20]</sup>。

与mTLE-HS相比,mTLE-OL患者对侧中央后回mALFF值减弱,即mTLE-HS在该区域癫痫活动更明显。中央后回与海马存在非直接突触连接,但SPECT显像显示其高灌注且皮质变薄<sup>[21]</sup>,可以解释为癫痫波传播的兴奋性毒性引起传入神经阻滞。相关分析提示,患者正激活区域(双侧扣带中后回)mALFF值与病程呈正相关,提示随着病程延长,该区域神经自发性活动更活跃;而负激活区域(双侧前扣带回)mALFF值与病程呈负相关,即癫痫波对该区域脑活动之抑制程度随着时间的延长而逐渐增强,提示癫痫早期诊断与治疗的重要性。

虽然两组癫痫患者的病灶位置有所不同,但均集中于内侧颞叶,并在数据处理中被mask遮盖。本研究侧重观察患侧颞叶外脑区,且ALFF值反映局部脑活动,而非各脑区功能连接,因此病灶位置差异对结果产生的影响极其微弱。综上所述,采用基

于ALFF的fMRI技术发现,不同病理基础内侧颞叶癫痫其脑功能活动改变的分布模式不同,二者为不同的疾病类型。mTLE-HS患者具有更广泛的脑活动异常区域,是一种特异性癫痫类型。本研究可为不同病理基础内侧颞叶癫痫的致痫灶定位和病理生理学机制阐述提供帮助。

## 参 考 文 献

- [1] Wieser HG; ILAE Commission on Neurosurgery of Epilepsy. ILAE commission report: mesial temporal lobe epilepsy with hippocampal sclerosis. *Epilepsia*, 2004, 45:695-714.
- [2] O'Brien TJ, Kilpatrick C, Murrie V, Vogrin S, Morris K, Cook MJ. Temporal lobe epilepsy caused by mesial temporal sclerosis and temporal neocortical lesions: a clinical and electroencephalographic study of 46 pathologically proven cases. *Brain*, 1996, 119(Pt 6):2133-2141.
- [3] Kerkhof M, Vecht CJ. Seizure characteristics and prognostic factors of gliomas. *Epilepsia*, 2013, 54 Suppl 9:12-17.
- [4] Ji GJ, Zhang Z, Zhang H, Wang J, Liu DQ, Zang YF, Liao W, Lu G. Disrupted causal connectivity in mesial temporal lobe epilepsy. *PLoS One*, 2013, 8:E63183.
- [5] Zang YF, He Y, Zhu CZ, Cao QJ, Sui MQ, Liang M, Tian LX, Jiang TZ, Wang YF. Altered baseline brain activity in children with ADHD revealed by resting - state functional MRI. *Brain Dev*, 2007, 29:83-91.
- [6] Matsumoto JY, Stead M, Kucewicz MT, Matsumoto AJ, Peters PA, Brinkmann BH, Danstrom JC, Goerss SJ, Marsh WR, Meyer FB, Worrell GA. Network oscillations modulate interictal epileptiform spike rate during human memory. *Brain*, 2013, 136(Pt 8):2444-2456.
- [7] Zhang Z, Lu G, Zhong Y, Tan Q, Chen H, Liao W, Tian L, Li Z, Shi J, Liu Y. fMRI study of mesial temporal lobe epilepsy using amplitude of low - frequency fluctuation analysis. *Hum Brain Mapp*, 2010, 31:1851-1861.
- [8] Zhang ZQ, Lu GM, Zhong Y, Tan QF, Zhu JG, Jiang L, Chen ZL, Wang ZQ, Shi JX, Zang YF, Liu YJ. Application of amplitude of low - frequency fluctuation to the temporal lobe epilepsy with bilateral hippocampal sclerosis: an fMRI study. *Zhonghua Yi Xue Za Zhi*, 2008, 88:1594-1598. [张志强, 卢光明, 钟元, 谭启富, 朱建国, 姜黎, 陈志立, 王中秋, 史继新, 谷玉峰, 刘一军. 低频振幅算法功能磁共振成像对双侧海马硬化颞叶癫痫的研究. 中华医学杂志, 2008, 88:1594-1598.]
- [9] Keller SS, O'Muircheartaigh J, Traynor C, Towgood K, Barker GJ, Richardson MP. Thalamotemporal impairment in temporal lobe epilepsy: a combined MRI analysis of structure, integrity, and connectivity. *Epilepsia*, 2014, 55:306-315.
- [10] Scanlon C, Mueller SG, Cheong I, Hartig M, Weiner MW, Laxer KD. Grey and white matter abnormalities in temporal lobe epilepsy with and without mesial temporal sclerosis. *J Neurol*, 2013, 260:2320-2329.
- [11] Zhang ZQ, Lu GM, Zhong Y, Tan QF, Tian L, Sun KJ, Shi JX. Changes in default-mode network connectivity in temporal lobe epilepsy: a functional MRI study. *Yi Xue Yan Jiu Sheng Xue Bao*, 2009, 22:36-43. [张志强, 卢光明, 钟元, 谭启富, 田雷, 孙康健, 史继新. 内侧颞叶癫痫患者脑缺省模式网络改变的功能MRI研究. 医学研究生学报, 2009, 22:36-43.]
- [12] Archer JS, Abbott DF, Waites AB, Jackson GD. fMRI "deactivation" of the posterior cingulate during generalized spike and wave. *Neuroimage*, 2003, 20:1915-1922.
- [13] Kay BP, DiFrancesco MW, Privitera MD, Gotman J, Holland

- SK, Szaflarski JP. Reduced default mode network connectivity in treatment-resistant idiopathic generalized epilepsy. *Epilepsia*, 2013, 54:461-470.
- [14] Jacobs J, Stich J, Zahneisen B, Asslander J, Ramantani G, Schulze-Bonhage A, Korinthenberg R, Hennig J, LeVan P. Fast fMRI provides high statistical power in the analysis of epileptic networks. *Neuroimage*, 2014, 88:282-294.
- [15] Fahoum F, Zelmann R, Tyvaert L, Dubeau F, Gotman J. Epileptic discharges affect the default mode network: fMRI and intracerebral EEG evidence. *PLoS One*, 2013, 8:E68038.
- [16] Chen ZL, Lu GM, Zhang ZQ, Tan QF, Zhong Y, Sun KJ, Tian L, Wang ZG, Zhu JG. Functional connectivity of hippocampus in mesial temporal lobe epilepsy: a functional magnetic resonance imaging study. *Zhongguo Xian Dai Shen Jing Ji Bing Za Zhi*, 2009, 9:355-360. [陈志立, 卢光明, 张志强, 谭启富, 钟元, 孙康健, 田蕾, 王正阁, 朱建国. 颞叶内侧癫痫海马功能连接的功能磁共振成像研究. 中国现代神经疾病杂志, 2009, 9: 355-360.]
- [17] Li JJ, Yang PJ, Jia JP. The cognitive difference of temporal lobe epilepsy patients between with and without hippocampal sclerosis. *Nao Yu Shen Jing Ji Bing Za Zhi*, 2007, 15:130-133. [李军杰, 杨培洁, 贾建平. 颞叶癫痫认知下降特点及其相关因素分析. 脑与神经疾病杂志, 2007, 15:130-133.]
- [18] Wang X, Yang N, He Y, Zhang Z, Zhu XT, Dong HM, Hou
- XH, Li HJ, Zuo XN. The developmental trajectory of hippocampus across the human lifespan based on multimodal neuroimaging. *Zhongguo Xian Dai Shen Jing Ji Bing Za Zhi*, 2014, 14:291-297. [王秀, 杨宁, 何叶, 张喆, 朱幸婷, 董昊铭, 侯晓晖, 李会杰, 左西年. 基于多模态神经影像学的人海马毕生变化曲线. 中国现代神经疾病杂志, 2014, 14:291-297.]
- [19] Kim JH, Im KC, Kim JS, Lee SA, Lee JK, Khang SK, Kang JK. Ictal hyperperfusion patterns in relation to ictal scalp EEG patterns in patients with unilateral hippocampal sclerosis: a SPECT study. *Epilepsia*, 2007, 48:270-277.
- [20] Wang MX, Zhang ZQ, Wang ZG, Shen LF, Lu GM. Study of amplitude of low frequency fluctuation in interictal epilepsy with generalized tonic clonic seizures based on fMRI. *Zhongguo Yi Xue Ying Xiang Ji Shu*, 2011, 27:1985-1989. [王茂雪, 张志强, 王正阁, 沈连芳, 卢光明. 全面强直阵挛癫痫发作间期的静息态fMRI低频振幅研究. 中国医学影像技术, 2011, 27: 1985-1989.]
- [21] Nelissen N, Van Paesschen W, Baete K, Van Laere K, Palmini A, Van Billoen H, Dupont P. Correlations of interictal FDG-PET metabolism and ictal SPECT perfusion changes in human temporal lobe epilepsy with hippocampal sclerosis. *Neuroimage*, 2006, 32:684-695.

(收稿日期:2014-09-24)

## · 小词典 ·

### 中英文对照名词词汇(六)

- 随机对照试验 randomized controlled trial(RCT)
- 髓鞘碱性蛋白 myelin basic protein(MBP)
- 锁核酸 locked nucleic acid(LNA)
- 胎牛血清 fetal bovine serum(FBS)
- 苔藓纤维出芽 mossy fiber sprouting(MFS)
- 特发性全面性癫痫 idiopathic generalized epilepsy(IGE)
- 梯度回波序列 gradient echo sequence(GRE)
- 同源性磷酸酶-张力蛋白 phosphatase and tensin homologue(PTEN)
- 铜锌超氧化物歧化酶 copper-zinc superoxide dismutase(Cu-ZnSOD)
- 酮戊二酸脱氢酶 oxoglutarate dehydrogenase complex(OGDC)
- 突触素 synaptophysin(Syn)
- 退化蛋白 degenerin(DEG)
- 托吡酯 topiramate(TPM)
- 微管相关蛋白 microtubule-associated protein(MAP)
- 微小RNA microRNA(miRNA)
- 无特定病原体 specific pathogen free(SPF)
- Cochrane系统评价数据库 The Cochrane Database of Systematic Reviews(CDSR)
- 细胞角蛋白 cytokeratin(CK)
- 细胞内结构域 intracellular domain(ICD)
- 细胞外基质 extracellular matrix(ECM)
- 细胞外结构域 extracellular domain(ECD)
- 纤溶酶原激活物抑制物-1 plasminogen activator inhibitor-1(PAI-1)
- 线粒体脑肌病伴高乳酸血症和卒中样发作 mitochondrial encephalopathy with lactic academia and stroke-like episodes(MELAS)
- 相位对比法 phase contrast(PC)
- 相位对比血管造影 phase contrast angiography(PCA)
- 新生儿肝内胆汁淤积症 neonatal intrahepatic cholestasis caused by Citrin deficiency (NICCD)
- 信号空间分割 signal space separation(SSP)
- 信噪比 signal-to-noise ratio(SNR)
- 兴奋性氨基酸转运蛋白 excitatory amino acid transporter(EAAT)
- 血管内皮生长因子 vascular endothelial growth factor(VEGF)
- 血管内皮生长因子受体 vascular endothelial growth factor receptor(VEGFR)
- 血氧水平依赖性功能磁共振成像 blood oxygenation level-dependent functional magnetic resonance imaging(BOLD-fMRI)
- 氧自由基 oxygen free radical(OFR)
- 夜发性额叶癫痫 nocturnal frontal lobe epilepsy(NFLE)
- 乙二胺四乙酸 ethylenediaminetetraacetic acid (EDTA)